European Journal of Pharmaceutical Sciences 48 (2013) 323–331

Contents lists available at SciVerse ScienceDirect

European Journal of Pharmaceutical Sciences

journal homepage: www.elsevier.com/locate/ejps

Oligochitosan polyplexes as carriers for retinal gene delivery

G. Puras [a,b,1], J. Zarate [a,b,1], A. Díaz-Tahoces [b,c], Marcelino Avilés-Trigueros [d], E. Fernández [b,c], J.L. Pedraz [a,b,*]

[a] NanoBioCel Group, University of Basque Country, Vitoria, Spain
[b] Networking Research Centre of Bioengineering, Biomaterials and Nanomedicine (CIBER-BBN), Spain
[c] Neuroprothesis and Neuroengineering Research Group, Miguel Hernández University, Spain
[d] Laboratory of Experimental Ophthalmology, Faculty of Medicine, University of Murcia, Regional Campus of International Excellence "Campus Mare Nostrum", Murcia, Spain

ARTICLE INFO

Article history:
Received 26 July 2012
Received in revised form 5 October 2012
Accepted 20 November 2012
Available online 29 November 2012

Keywords:
Non-viral gene therapy
Low molecular weight chitosan
Retina
Polyplexes
Gene delivery

ABSTRACT

Non-viral gene therapy represents a promising approach for the treatment of retinal diseases. However, the lack of an efficient carrier hampers the implementation of this therapy. In this study, we evaluated low molecular weight ultrapure oligochitosans for the delivery of the pCMS-EGFP plasmid into the rat retina cells after subretinal and intravitreal administrations. Polyplexes were technologically characterized. Resulting polyplexes based on ultrapure oligochitosans were slightly spherical, protected the plasmid against enzymatic digestion, and their charge and size values ranged from 8 to 14 millivolts and from 150 to 69 nm respectively depending on the *N*/*P* ratio. In HEK-293 cultured cells, transfection efficiency significantly increased from 12% to 30% when pH decreased from 7.4 to 7.1 (data normalized to Lipofectamine™ 2000). However, no significant transfection was detected in ARPE-19 cultured cells. Subretinal administrations transfected mainly the pigmented cells of the retinal pigment epithelium and the light sensitive photoreceptor cells, whereas intravitreal injections transfected cells in the ganglion cell layer, blood vessels in the inner layers of the retina and photoreceptors. These results support the potential use of oligochitosans for delivering genetic material into retinal cells *in vivo*.

© 2012 Elsevier B.V. All rights reserved.

1. Introduction

Gene therapy represents a powerful approach to produce bioactive agents, replace defective genes or modulate unwanted gene expression by delivering genetic material into the nucleus of specific cells. The most basic vehicle for non-viral gene therapy is naked DNA. However, DNA is rapidly degraded by nucleases, showing poor cellular uptake and low transfection efficiency. Therefore, the development of an effective carrier for therapeutic plasmids remains a central challenge for gene therapy success (Rolland, 2005). At present, most gene delivery systems use viral or non-viral vectors. Among the different viral vectors, the adeno-associated virus (AAV) based vectors have emerged as the gold standard for the treatment of the Lebeŕs congenital amaurosis (LCA), which is an inherent eye disease caused by mutations in the REP-specific 65 kDa protein, encoded by the RPE65 gene. First human clinical trial results were published in 2008 (Bainbridge et al., 2008; Cideciyan et al., 2008; Hauswirth et al., 2008; Maguire et al., 2008). Nowadays, and after the initial thriving and encouraging results, many clinical trials related to viral approaches, gene therapy and RPE65 mutations are in progress (http://clinicaltrials.gov/). However, viral vectors generally suffer from important safety issues such as insertional muta-genesis, toxicity and immunogenicity. In addition, the high production cost and the small size of the DNA they can transport (except newer adenoviral vectors) have motivated the need to develop safer and less cytotoxic vectors (Jafari et al., 2012). Consequently, research on non-viral vectors has gained momentum, as they do not exhibit antigen-specific immune and inflammatory response, are cheaper to produce and the size of inserted DNA is theoretically unlimited (Charbel Issa and MacLaren, 2012). However, their low transfection efficiency represents the most important limitation for clinical applications. Therefore, research on non-viral retinal gene delivery merits investigation, since represents a promising approach to deliver genetic material into the retina.

The eye is a promising immune-privileged organ for non-viral gene therapy because its compartmentalized anatomy permits localized delivery to specific ocular tissues and it is affected by many well understood genetic-based diseases. Furthermore, as the media is transparent, the gene transfer process can be easily tracked, and the small volume of the tissue to be treated decreases the doses needed for therapeutic effects, minimizing the potential adverse reactions (Liu et al., 2011). Hence, since the 1990s, there has been a growing interest in exploring the suitability of non-viral gene delivery systems for ocular therapy purposes (Diebold and Calonge, 2010; Nussenblatt and Csaky, 1997), and specifically, for

* Corresponding author. Address: Laboratory of Pharmacy and Pharmaceutical Technology, Faculty of Pharmacy, University of the Basque Country, 01006 Vitoria-Gasteiz, Spain. Tel.: +34 945013091; fax: +34 945013040.
E-mail address: joseluis.pedraz@ehu.es (J.L. Pedraz).
[1] These authors contributed equally to this work.

0928-0987/$ - see front matter © 2012 Elsevier B.V. All rights reserved.
http://dx.doi.org/10.1016/j.ejps.2012.11.009

chronic posterior segment diseases that affect the retina such as age-related macular degeneration, retinitis pigmentosa or cytomegalovirus retinitis (Charbel Issa and MacLaren, 2012). The major chemical non-viral carriers used for gene delivery to retinal cells *in vivo* are peptides (Johnson et al., 2008), liposomes (Zhang et al., 2003), solid lipid nanoparticles (Delgado et al., 2012) and polymers (Bejjani et al., 2005). Among polymers, oligochitosan-based formulations have recently been evaluated as promising gene carrier on the ocular surface (Klausner et al., 2010, 2012); however, according with our knowledge, there are no reports about the efficiency of oligochitosans as gene carrier for retinal cells.

We designed polyplexes based on NOVAFECT O25 oligochitosans, an ultrapure and highly deacetylated oligochitosans that easily form polyplexes with DNA through electrostatic interactions (Klausner et al., 2010), and characterized them by cryogenic-transmission electron microscopy (Cryo-TEM) and by their ability to complex and protect the plasmid DNA from deoxyribonuclease I (DNase I) enzymatic digestion on agarose gel electrophoresis assays. Hydrodynamic size diameter and surface charge density of polyplexes were evaluated at *N*/*P* ratios from 10 to 60, and best formulations were selected for *in vitro* transfection studies at pH 7.4 and 7.1, since it has been widely reported that chitosan-mediated transfection efficiency strongly depends on slight changes in the pH value of the transfection medium (Nimesh et al., 2010; Sato et al., 2001). In addition, humor vitreous pH value is approximately 7.1 (Bassnett and Duncan, 1985), slightly more acid than either plasma or aqueous humor. *In vitro* transfection experiments were done on the well known model for transfection studies, the human embryonic kidney cell line (HEK-293), and in a cell line of the retina more difficult to be transfected, the human retinal epithelium pigment cell line (ARPE-19), which plays a major role in ocular diseases associated with senescence and dystrophies of the photoreceptors (Bejjani et al., 2005). In order to elucidate the potential application of oligochitosans as DNA carriers for the retina, we administered the polyplexes based on oligochitosans by subretinal and intravitreal injections, which are the most widely routes employed to deliver genetic material into the posterior segment of the eye, and evaluated the expression of the enhanced green fluorescent protein (EGFP) at 72 h in different cells and layers of the retina.

2. Materials and methods

2.1. Materials

NOVAFECT O25 oligochitosan acetate salt, with a molecular weight (MW) of 7.3 kDa, a degree of deacetylation (DDA) $\geqslant$ 97%, and endotoxin levels $\leqslant$ 0.05 EU/mg, was purchased from NovaMatrix/FMC (Sandvika, Norway). HEK-293 cells, ARPE-19 cells and Eaglés Minimal Essential medium with Earlés BSS and 2 mM l-glutamine (EMEM) were obtained from the American Type Culture Collection (ATCC). Dulbeccós Modified Eaglés Medium Hańs Nutrient Mixture F-12 (1:1) medium was purchased from GIBCO (San Diego, California, US). The plasmid pCMS-EGFP, which encodes the EGFP, was purchased from BD Biosciences Clontech (Palo Alto, California, US) and amplified by Dro Biosystems S.L. (San Sebastian, Spain). The gel electrophoresis materials and ethidium bromide solution were acquired from Bio-Rad (Madrid, Spain). DNase I, lauryl sulfate sodium (SDS), PBS, HEPES, MES and sodium bicarbonate reagent were purchased from Sigma–Aldrich (Madrid, Spain). Opti-MEM® I reduced medium, antibiotic/antimicotic solution and Lipofectamine™ 2000 transfection reagent were acquired from Invitrogen (San Diego, California, US). The BD Viaprobe kit was provided by BD Biosciences (Belgium). Adult Sprague–Dawley rats were purchased from Harlan Laboratories (Barcelona, Spain).

2.2. Preparation of oligochitosan/DNA polyplexes

Oligochitosan/DNA polyplexes having a DNA concentration of 13.2 μg/ml at different *N*/*P* ratios were prepared by the self-assembly method. Briefly, the DNA stock solution was diluted in ultrapure water and the chitosan stock solution was added to the plasmid DNA water mixture under vortex mixing (1200 rpm) for at least 10 s, and subsequently equilibrated at room temperature for 30 min before performing transfection experiments. An example of a series of formulations of oligochitosan/DNA polyplexes is shown in Table 1.

2.3. Cryo-TEM microscopy

Oligochitosan/DNA polyplexes were observed by Cryo-TEM microscopy. Briefly, one drop of the sample solution was vitrified by rapid freezing in liquid ethane using a Vitrobot Markt IV (FEI, Eindhoven, The Netherlands). This vitrified sample grid was transferred through 655 Turbo Pumping Station (Gatan, France) to a 626 DH Single Tilt Liquid Nitrogen Cryo-holder (Gatan, France), where it was maintained at about −180 °C. Copper grid (300 mesh Quantifoils) was hydrophilized by glow-discharge treatment. The sample was examined in a Transmission Electron Microscope, TECNAI G2 20 TWIN (FEI, Eindhoven, The Netherlands), operating at an accelerating voltage of 200 keV in a bright-field and low-dose image mode.

2.4. Measurements of size and zeta potential

The hydrodynamic diameter of the polyplexes was determined by dynamic light scattering (DLS). Briefly, polyplexes (100 μl) were resuspended into HEPES medium (1400 μl, 10 mM, pH 7.1) and size was determined using Zetasizer Nano ZS (Malvern Instruments, UK). All measurements were carried out in triplicate. The particle size reported as hydrodynamic diameter was obtained by cumulative analysis.

Zeta potential measurements were obtained by laser doppler velocimetry (LDV) after resuspending the polyplexes (100 μl) into HEPES medium (1400 μl, 10 mM, pH 7.1) using folded capillary cells for zeta analysis. The Smoluchowski approximation was used to support the calculation of the zeta potential from the electrophoretic mobility. Zeta potential measurements were run in triplicate. Only data that met the quality criteria according with the software programme (DTS 5.0) were included in the study.

2.5. Gel retardation assay

The capacity of oligochitosans to complex, release and protect DNA from DNase I enzymatic digestion was estimated by agarose gel electrophoresis assays. Naked DNA or samples of polyplexes at an *N*/*P* ratio from 10 to 60 (20 μl, containing 200 ng of the plasmid) were loaded to an agarose gel (0.8%) that contained 1% of ethidium bromide for visualization. The gel was immersed in a tris–acetate-EDTA buffer and exposed for 30 min to 120 V. Bands were observed with a model TFX-20 M transilluminator (Vilber-Lourmat, Germany), and the images were captured using a digital camera from BioRad, DigiDoc model. To estimate the capacity of polyplexes to release DNA, 20 μl of a 2% SDS solution was added to the samples resulting in a final concentration of 1%. Protection capacity of the polyplexes against enzymatic digestion was studied after adding DNase I (final concentration 1 U DNase I/2.5 μg DNA). Afterwards, the mixtures were incubated at 37 °C for 30 min. Finally, 2% SDS solution was added to release DNA from polyplexes. The

Table 1
Oligochitosan/DNA polyplexes formulations with a DNA concentration of 13.2 μg/ml at different *N*/*P* ratio[a].

N/*P* ratio	Plasmid (0.5 mg/ml) (μl)	NOVAFECT (2 mg/ml) (μl)	Ultrapure water (μl)	Total volume (μl)
10	13.2	22.1	464.7	500
20	13.2	44.2	442.6	500
30	13.2	66.5	420.3	500
40	13.2	88.4	398.4	500
50	13.2	110.5	376.3	500
60	13.2	133	358.8	500

[a] If a concentration of plasmid DNA higher than 13.2 μg/ml is required, manufacteŕs protocol recommends mixing NOVAFECT O25 oligochitosan reagent and plasmid DNA in approximately 1:1 (v/v) ratio to avoid aggregation.

integrity of the DNA in each sample was compared with untreated DNA.

2.6. In vitro transfection

HEK-293 and ARPE-19 cells were seeded in 24-well plates at an initial density of 15×10^4 and 10×10^4 cells/well, with 1 ml EMEM containing 10% horse serum and with 1 ml D-MEM/F-12 containing 10% fetal calf serum, respectively. Then, the regular growth media was removed and the cells were exposed to polyplexes containing 1.65 μg of the plasmid and adequate amounts of oligochitosans (see Table 1). Formulations for transfection were prepared after mixing 1:1 oligochitosan polyplexes and hypertonic (580 mM) serum-free transfection medium (Opti-MEM® I, pH 7.4 containing 270 mM mannitol), so that the final formulation is isotonic. Cells were then carefully washed with PBS, and 250 μl of the transfection formulation was added to each well. Each formulation was used in triplicate for statistical analysis. After 4 h of incubation at 37 °C, the transfection medium was replaced by 500 μl of regular growth medium. Cells were allowed to grow for 72 h until fluorescent microscopy and flow cytometry analysis. Transfection experiments at pH 7.1 were performed as above, except of the addition of 10 mM HEPES to the hypertonic serum-free Opti-MEM® I transfection medium. The pH value of the transfection medium was adjusted with 1 N HCl during the same day of the transfection and filtered with Millipore 0.22 μm PVC filters (Madrid, Spain). After 4 h of incubation at 37 °C, the transfection medium (pH 7.1) was replaced by 500 μl of regular growth medium, pH 7.4, and cells were allowed to grow until florescent microscopy and flow cytometry assays (72 h). Experiments with Lipofectamine™ 2000/pDNA lipoplexes were prepared following the manufacturer's protocol.

Qualitative expression of EGFP was examined 72 h post-transfection using an inverted microscope with simultaneous epi-fluorescence and phase contrast observation (Eclipse TE200-S, Nikon Instruments Europe B.V., Amstelveen, The Netherlands). Images were captured with a 20× objective. Afterwards, flow cytometry analysis was conducted on a FACSCalibur system flow cytometer (Becton Dickinson Biosciences, San Jose, USA) in order to quantify the EGFP expression. Cells were washed twice in PBS and detached from the microplate with 300 μl of 0.05% trypsin/EDTA. Then, cells were centrifuged and the supernatant was discarded. The pellet was resuspended in PBS, diluted in FACSFlow liquid and directly introduced to the flow cytometer. Transfection efficiency was expressed as the percentage of EGFP positive live cells at 525 nm (FL_1). For cell viability measurements, the BD-via Probe reagent (5 μL) was added to each sample. BD-via Probe positive cells were excluded from the EGFP expression analysis. The fluorescence corresponding to dead cells was measured at 650 nm (FL_3). Control samples (non-transfected cells) were displayed on a forward scatter (FSC) versus side scatter (SSC), dot plot to establish a collection gate and exclude cells debris. Other samples containing Lipofectamine transfected cells without BD-via Probe, and non-transfected cells with BD-via Probe were used as controls to compensate FL_2 signal in FL_1 and FL_3 channels. For each sample 10,000 events were collected.

2.7. Animals and anesthetics

Adult male Sprague Dawley rats (6–7 weeks old and 150–200 g body weight) were used as experimental animals. Rats were housed in temperature and light controlled rooms with a 12 h light/dark cycle and had food and water ad libitum. All experimental procedures were carried out in accordance with the Spanish and European Union regulations for the use of animals in research and the Association for Research in Vision and Ophthalmology (ARVO) statement for the use of animals in ophthalmic and vision research and supervised by the Miguel Hernandez University Standing Committee for Animal Use in Laboratory. Adequate measures were taken to minimize pain or discomfort. All the experimental manipulations were carried under general anesthesia induced with an intraperitoneal (i.p.) injection of a mixture of ketamine (70 mg/kg, Ketolar®, Parke–Davies, S.L., Barcelona, Spain) and xylazine (10 mg/kg, Rompún®, Bayer, S.A., Barcelona, Spain). For recovery from anesthesia, rats were placed in their cages and an ointment containing tobramycin (Tobrex® pomada oftálmica, Alcon S.A., Barcelona, Spain) was applied on the cornea to prevent corneal desiccation. Animals were sacrificed by an i.p. injection of an overdose of 20% sodium pentobarbital (Dolethal Vetoquinol®, Especialidades Veterinarias, S.A., Alcobendas, Madrid, Spain).

Animals were randomly divided into three groups ($n = 4$ each) and received by intravitreal or subretinal route a solution of naked plasmid (100 ng) or a suspension based on oligochitosan polyplexes with an *N*/*P* ratio of 10 or 30 containing 100 ng of the plasmid. Polyplexes and plasmid were diluted in a total volume of 5 μl of 10 mM HEPES medium and the pH was adjusted to 7.1 in sterile conditions before injections.

2.8. Intravitreal and subretinal administration

Under an operating microscope (Zeiss OPMI® pico; Carl Zeiss Meditec GmbH, Jena, Germany) and after piercing the conjunctiva and sclera on the left eye superotemporal region with a 30-gauge needle, a single 4 μl administration of the suspensions was performed with the aid of a 5 μl Hamilton microsyringe (Hamilton Co., Reno, NV). A bent 34-gauge needle was used to inject into the vitreous of the left eye, immediately adjacent to the ora serrata without touching the lens. The right advancement of the needle was directly observed. In order to deliver the suspension into the subretinal space the needle was passed through the sclerotomy 2 mm posterior to ora serrata and in a tangential direction toward the posterior retinal pole along the subretinal space. Successful administration of suspensions into the subretinal space was confirmed by the appearance of a partial retinal detachment by direct ophthalmoscopy of the eye fundus through the operating microscope. As for all the rats, the untreated right eye, which had not been manipulated, served as a normal counterpart or control.

Seventy-two hours post-injection, the rats from each experimental group (DNA treated group, and groups treated with oligochitosan polyplexes at *N*/*P* ratios of 10 or 30) were sacrificed as described above and perfused transcardially with 0.9% saline followed by 4% paraformaldehyde in 0.1 M phosphate buffer (pH 7.2–7.4) at 4 °C.

2.9. Evaluation of EGFP expression in rat retinas

For whole-mount preparations, both eyes from two rats of each group were enucleated and immersed for 1 h in a solution of 4% paraformaldehyde in PBS. Later, the retinas were dissected as wholemounts by making four radial cuts in the superior, inferior, nasal, and temporal retinal poles. Retinal orientation was maintained by making the deepest radial cut in the superior retina. The retinas were postfixed for 1 h in the same fixative, rinsed in PBS, and mounted vitreal side up on poly-L-lysine coated microscope slides, covered with anti-fading mounting media containing 50% glycerol and 0.04% *p*-phenylenediamine in 0.1 M sodium carbonate buffer (pH 9.0).

For sagital section preparations, both eyes from two rats of each group were enucleated, and the anterior segments, including the lens, were removed. Posterior eyecups were fixed for 1 h with 4% paraformaldehyde in 0.1 M PBS, followed by several washes in PBS. Samples were then immersed in 30% sucrose in PBS overnight at 4 °C for cryoprotection. Eyecups were embedded and oriented in optimal cutting temperature (O.C.T.™) compound (Tissue-Tek®; Sakura Finetek Europe B.V., Alphen and den Rijn, The Netherlands) and frozen in 2-methylbutane cooled in liquid nitrogen at −60 °C. Radial sections (15 μm) were cut with a cryostat (HM 550; Microm International GmbH, Walldorf, Germany), mounted on SuperFrost® Plus microscope slides (VWR International bvba, Leuven, Belgium). To counterstain all retinal nuclei, sections were stained with 5 μg/ml Hoechst 33342 dye (Sigma–Aldrich) for 5 min and then thoroughly washed with PBS 0.1 M and covered with anti-fading mounting media.

EGFP expression and DAPI staining were evaluated with the help of a Leica TCS SPE spectral confocal microscope.

2.10. Statistical analysis

Statistical analysis was completed with the InStat programme (GraphPad Software, San Diego, CA, USA). Differences between groups at significance levels of 95% were calculated by the Student's *t* test. In all cases, *P* values <0.05 were regarded as significant. Normal distribution of samples was assessed by the Kolmogorov–Smirnov test, and the homogeneity of the variance by the Levene test. Data were presented as mean ± SD, unless stated otherwise.

3. Results

3.1. Cryo-TEM characterization

The morphology and size of the oligochitosan/DNA polyplexes were assessed by Cryo-TEM microscopy. Fig. 1 shows a heterogeneous population of slightly spherical nature with a particle diameter clearly inferior to 500 nm, in agreement with the DLS characterization in Fig. 2.

3.2. Measurements of size and zeta potential

Fig. 2 represents the size and the zeta potential of polyplexes. The size was clearly affected by the *N*/*P* ratio, since the highest values were obtained at *N*/*P* ratio of 10 (150 nm) whereas the lowest values were obtained at *N*/*P* ratio of 50 (69 nm), although a slight increase in the size was observed at *N*/*P* ratio of 60 (86 nm). In all cases, polydispersity index was below 0.3 (data not shown). Regarding to zeta potential, the lowest values were obtained at *N*/*P* ratio of 10 (8 mV), whereas the highest values were reached at high *N*/*P* ratio of 40 (14 mV). At *N*/*P* ratios of 50 and 60, zeta potential decreased to 12 mV.

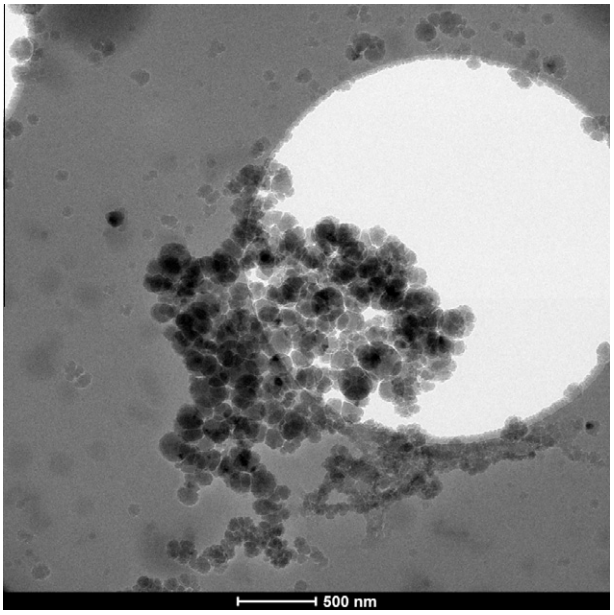

Fig. 1. Cryo-TEM image of oligochitosan/DNA polyplexes, *N*/*P* = 10, suspended in HEPES medium 10 mM, pH 7.1.

3.3. Agarose gel electrophoresis assays

Fig. 3 represents the electrophoresis assay to determine the binding efficiency between oligochitosan and DNA, and the capacity of the chitosans to protect the DNA against enzymatic digestion at different *N*/*P* ratios. The absence of signal in lane 3 suggests that the enzyme worked properly. From Fig. 3 we can observe that our formulations were able to complex, release and protect the plasmid, depending on the *N*/*P* ratio used to elaborate the polyplexes.

3.4. Transfection efficiency and cell viability in HEK-293 cells

Transfection efficiency was evaluated quantitatively by flow cytometry and qualitatively by fluorescent microscopy to study the influence of both *N*/*P* ratio and pH. As can be observed from the phase contrast and fluorescent images obtained by microscopy, the transfection efficiency of cells treated with oligochitosan/DNA polyplexes at *N*/*P* ratio of 10 and pH 7.4 (Fig. 4B1 and B2) was clearly inferior to that obtained at the same *N*/*P* ratio at pH 7.1 (Fig. 4C1 and C2). However, the greatest EGFP expression was obtained when cells were transfected with Lipofectamine™ 2000 (Fig. 4D1 and D2). Flow cytometry FL_1/FL_3 dot plots in Fig. 4B3 (polyplexes at *N*/*P* ratio of 10, pH 7.4), Fig. 4C3 (polyplexes at *N*/*P* ratio of 10, pH 7.1) and Fig. 4D3 (Lipofectamine™ 2000), corroborated the microscopy images and allowed us to quantify the transfection efficiency and cell viability in terms of percentage of transfected and viable cells. In Fig. 4A (bars), can be appreciated that at pH 7.4 the percentage of transfected cells ranged between 8% at *N*/*P* ratio of 10% and 12% at *N*/*P* ratio of 30; however at pH 7.1 the percentage of transfected cells increased significantly ($p < 0.0001$, for all *N*/*P* ratios). Values ranged between 30% and

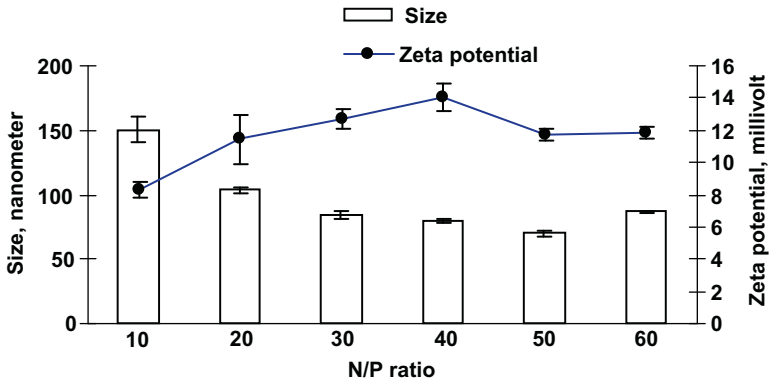

Fig. 2. Effect of *N*/*P* ratio on size and zeta potential of oligochitosan/DNA polyplexes suspended in HEPES medium 10 mM, pH 7.1 (mean ± SD, $n = 3$).

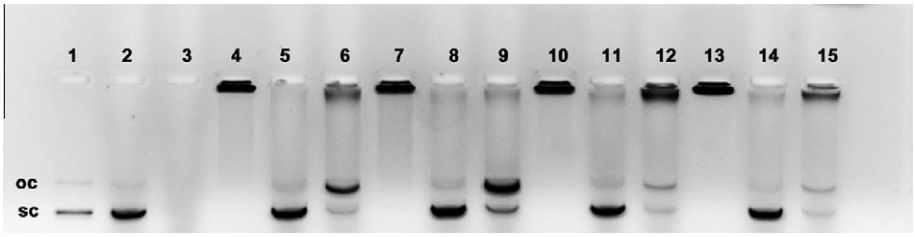

Fig. 3. Binding efficiency between the oligochitosan and the DNA at different *N*/*P* ratios, and protection capacity from DNase I enzymatic digestion visualized by agarose gel electrophoresis. OC: open circular form, SC: supercoiled form. Lanes 1–3 correspond to free DNA; lanes 4–6, *N*/*P* 5; lanes 7–9, *N*/*P* 10; lanes 10–12, *N*/*P* 20; lanes 13–15, *N*/*P* 30. Polyplexes were treated with SDS (lanes 2, 5, 8, 11 and 14) and SDS + DNase I (lanes 3, 6, 9, and 15).

24% at *N*/*P* ratios of 10 and 20, respectively (all data were normalized to Lipofectamine™ 2000). Cell viability always was over 90% at both pH values. In summary, a significant enhancement in transfection efficiency of the oligochitosan/DNA polyplexes was achieved when the pH of the transfection medium slightly decreased from 7.4 to 7.1.

3.5. Transfection efficiency and cell viability in ARPE-19 cells

As in HEK-293 cells, we evaluated the effect of the pH on both transfection efficiency and cell viability when polyplexes were administered at different *N*/*P* ratios to ARPE-19 cells *in vitro*. In our hands, oligochitosans did not efficiently transfect ARPE-19 cells neither at pH 7.4 nor at pH 7.1, while Lipofectamine™ 2000 modestly transfected ARPE-19 cells (20%, data not shown). Regarding cell viability, we observed that the viability of the cells treated with polyplexes was over 90% for all *N*/*P* tested, however, a drastically decrease in the viability, more than 50%, was observed when cells were treated with Lipofectamine™ 2000 (data not shown).

3.6. EGFP expression after subretinal injection

In order to evaluate the transfection efficiency after subretinal administration, a DNA solution and two formulations of the polyplexes at *N*/*P* ratios of 10 and 30 were injected, and rat retinas were processed 72 h later for EGFP visualization (Fig. 5A). Significant EGFP expression was detected only in the group treated with oligochitosan/DNA polyplexes at *N*/*P* ratio of 10 (Fig. 5B–D). No gene expression was observed after the administration of the DNA solution, and little-to-no transfection was detected with the polyplexes at *N*/*P* ratio of 30 (data not shown). High levels of EGFP expression were detected mainly in the outer segments of the photoreceptors (Fig. 5B and C) and in the retinal pigment epithelium (RPE) layer, but we also found EGFP expression in Müller cells and blood vessels (Fig. 5C). When rat retinas were whole-mounted processed (Fig. 5D), an important number of transfected cells were detected in the RPE layer.

3.7. EGFP expression after intravitreal injection

We injected into the vitreous two formulations based on oligochitosan/DNA polyplexes at *N*/*P* ratio of 10 and 30, and a naked DNA solution to evaluate the transfection efficiency in different layers of the rat retina 72 h post injection. No gene expression was observed after the administration of the DNA solution (data not shown). Transfected cells after polyplexes administration were only detected at *N*/*P* ratio of 10. There was substantial transfection of inner layers of the retina (Fig. 6A–C). Close examination revealed significant transfection of blood vessels, and retinal ganglion cells (Fig. 6B and C). Surprisingly, significant transfection was also found in the inner layers of the retina but also in the outer segments of the photoreceptors and RPE (Fig. 6B and C).

4. Discussion

The current study was designed to evaluate the potential use of ultrapure oligochitosans for delivering genetic material into the rat retina. A selected formulation of polyplexes based on oligochitosans led to a significant EGFP expression in different layers and cells, depending strongly on the administration route.

Polyplexes based on ultrapure oligochitosans were prepared by the self assembly method (Klausner et al., 2010) and the morphology was visualized using Cryo-TEM, since it has been widely reported that the analysis of the final structure is necessary for an efficient evaluation of gene delivery vectors (Danielsen et al., 2004; Maurstad et al., 2007). Morphology of chitosan/DNA polyplexes may exhibit different structures such as rods, spheres, toroids or globules, depending not only on the characteristics of the polyplexes (chitosan, plasmid, *N*/*P* ratio) but also on the properties of the solution (ionic strength, pH). As observed from Fig. 1, most of

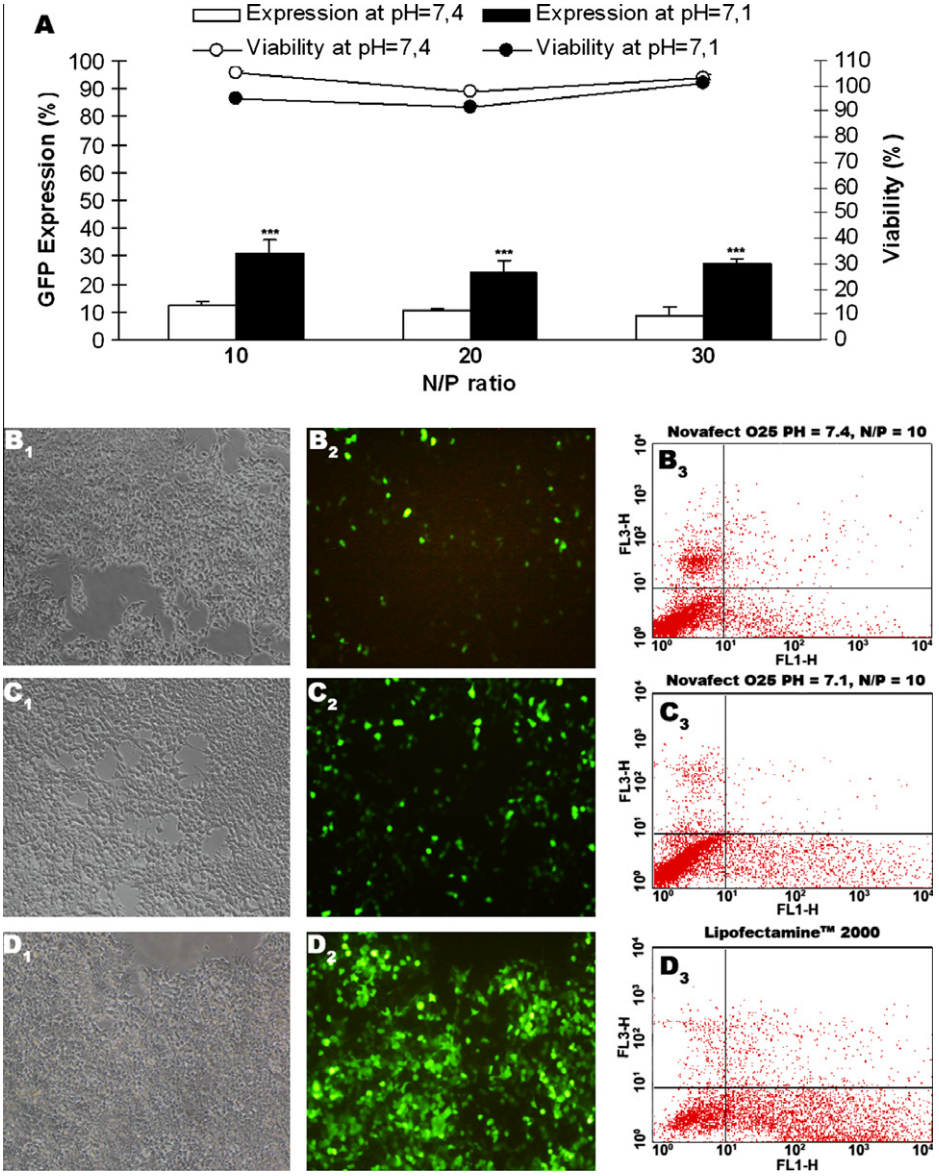

Fig. 4. Transfection efficiency of oligochitosan/DNA polyplexes in HEK-293 cells. (A) Influence of *N*/*P* ratio and pH on EGFP expression and cell viability. Transfection data were normalized to Lipofectamine™ 2000 (mean ± SD; $n = 3$). EGFP expression at pH 7.4 was significantly higher than at pH 7.1at all *N*/*P* ratio studied, $^{***}P < 0.0001$. At all *N*/*P* ratio tested, statistical differences were reached when compared the EGFP expression at pH 7.4 and 7.1, $^{***}P < 0.0001$. (B_1) Phase contrast image, (B_2) fluorescent image and (B_3) flow cytometry dot-plot (FL_1/FL_3) of HEK-293 cells transfected with polyplexes at pH 7.4 and *N*/*P* ratio 10. (C_1) Phase contrast image, (C_2) fluorescent image, and (C_3) flow cytometry dot-plot (FL_1/FL_3) of HEK-293 cells transfected with polyplexes at pH 7.1 and *N*/*P* ratio 10. (D_1) Phase contrast image, (D_2) fluorescent image, and (D_3) flow cytometry dot-plot (FL_1/FL_3) of HEK-293 cells transfected with Lipofectamine™ 2000. Images were acquired at 3 days post-transfection, original magnification 20×.

the polyplexes formed were slightly spherical in shape when suspended in HEPES medium 10 mM, pH 7.1 at *N*/*P* ratio of 10.

Under all *N*/*P* ratios used, the particle size was in the nano-range (Fig. 2). It has been reported that compared with microparticles, particles in the nanometer range have a higher intracellular uptake (Bivas-Benita et al., 2004), which strongly contributes to enhance transfection efficiency (Huang et al., 2005). Particle size of polyplexes based on chitosan polymers may be affected by different parameters including the preparation method, the characteristics of the chitosan, such as MW and DDA, the buffer composition (pH, ionic strength) or the *N*/*P* ratio (Danielsen et al., 2004; Mao et al., 2001; Nimesh et al., 2010).

In our experimental conditions, particle size of polyplexes was inversely proportional to the charge ratio, with values ranging from 150 nm at *N*/*P* ratio of 10–70 nm at *N*/*P* ratio of 50. The reduction of the particle size at high *N*/*P* ratios can be attributed to the ability of the oligochitosan to precondense DNA; however, when *N*/*P* increased to 60, particle size increased to 86 nm. Such increase may be caused by the greater demand of space that high *N*/*P* ratios require. Therefore, it seems that a delicate balance between the ability of the oligochitosan to condense the plasmid and the greater space demanded by itself determines modifications on the final particle size.

Regarding the surface charge of the polyplexes (Fig. 2), all *N*/*P* ratios studied had positive zeta potentials, due to the presence of protonated amino groups of oligochitosan that were not neutralised by the negative charges of the plasmid. A final positive charge on the surface of the polyplexes enhances electrostatic interactions with negatively charged cellular membranes (Huang et al., 2005) and the posterior uptake through the cell membrane (Dias et al., 2002). In our experimental conditions, zeta potential varied from 8 mV at *N*/*P* ratio of 10–14 mV at *N*/*P* ratio of 40, suggesting that

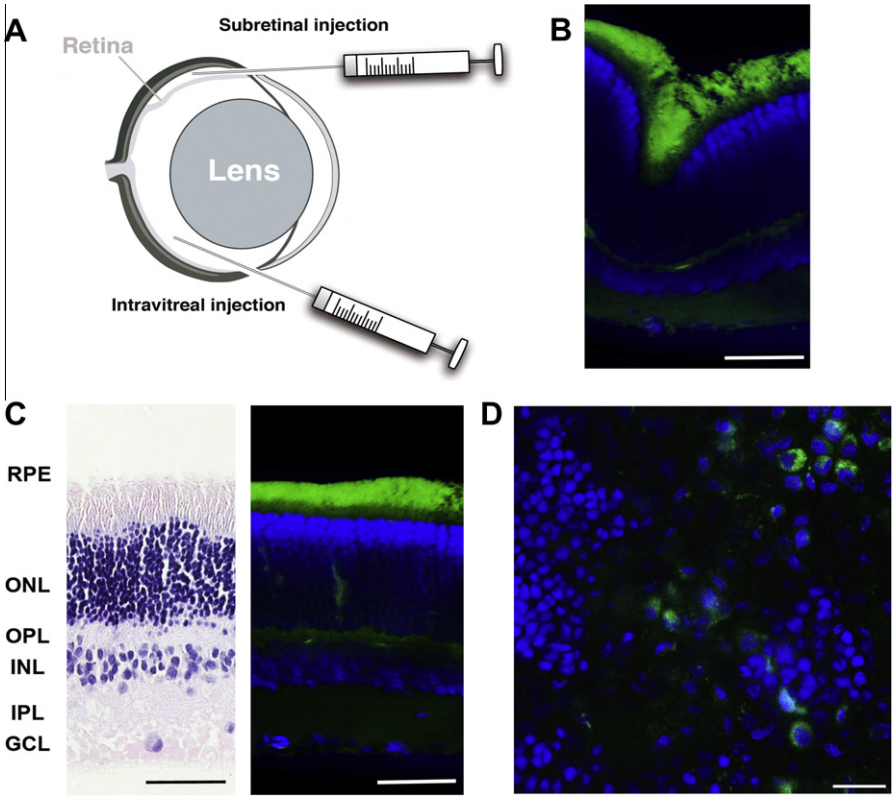

Fig. 5. *In vivo* gene expression of EGFP after administration of oligochitosan/DNA polyplexes at *N*/*P* ratio of 10 to rats. (A) Schematic drawing of the subretinal and intravitreal injection. (B) Cross-section of a treated retina close to the place of the subretinal injection. EGFP expression with Hoechst 33342 staining for cell nuclei. Scale bar = 50 μm. (C) Hematoxylin-eosin rat retina cross-section, showing the different layers of the retina. RPE (Retinal Pigment Epithelium layer), ONL (Outer nuclear layer), OPL (Outer plexiform layer), INL (Inner nuclear layer), IPL (Inner plexiform layer), GCL (Ganglion cell layer) and fluorescent microscopy image of a 5-μm treated retina cross-section. Scale bar = 50 μm. (D) Whole-mount views of several sections of the retina focused at the RPE layer. Scale bar = 100 μm.

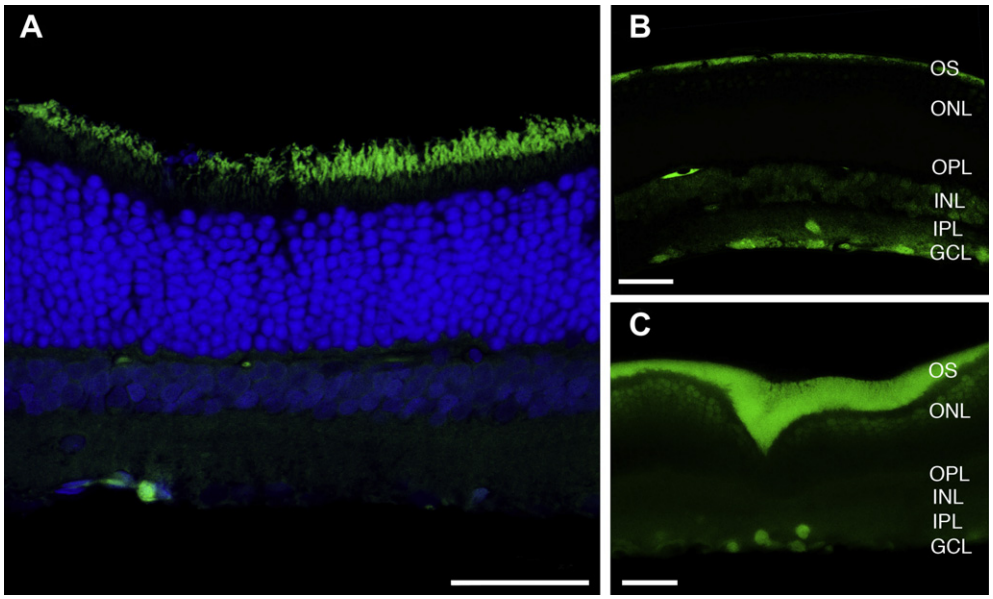

Fig. 6. *In vivo* gene expression of EGFP after intravitreal administration of plasmid DNA and oligochitosan/DNA polyplexes at an *N*/*P* ratio of 10 to rats. (A) Fluorescent microscopy image of a treated retina cross-section. EGFP expression was localized mainly at the inner layers of the retina and outer segments of the photoreceptors. Blue, Hoechst 33342 staining for cell nuclei. (B and C) Cross-sections of treated sections of retinas without Hoechst 33342 staining. Scale bars = 50 μm.

zeta potential is directly proportional to charge ratio. However, at *N*/*P* ratio of 50, there was a steady-state for zeta potential value (Kiang et al., 2004; Mao et al., 2001) since values at *N*/*P* ratio of 50 and 60 were quite similar (around 12 mV). Zeta potential values strongly depend not only on the characteristics of the chitosan (MW, DDA) but also on the pH and ionic strength of the medium (Nimesh et al., 2010). Therefore, these parameters should be considering when analyzing zeta potential to make studies more com-

parable. In addition, calculation parameters should be explained as well, since they strongly affect to the final value.

One critical parameter of DNA delivery systems to transfect cells efficiently cells is the ability of the carrier material to condense, and protect incorporated plasmid against enzymatic degradation. In addition, a delicate balance between DNA binding capacity and DNA release must be achieved since transfection efficiency is hampered by great binding strengths between chitosan and plasmid (Alatorre-Meda et al., 2011). Fig. 3 shows that at all *N*/*P* ratios, oligochitosans were able to condense plasmid DNA, since no plasmid DNA migration was observed. Furthermore, when SDS was added to release the condensed plasmid DNA, the plasmid migrated at all *N*/*P* ratios tested, which suggests a weak chitosan-DNA binding affinity, although on lanes 11 (*N*/*P* ratio of 20) and 14 (*N*/*P* ratio of 30) a small amount of DNA still remains bound to the oligochitosans, indicating stronger binding affinity as *N*/*P* ratio increases, probably because polyplexes are more positively charged (Fig. 2). Interestingly, all *N*/*P* ratios protected the plasmid against DNase I enzymatic digestion, although the most intensive signal of the supercoiled form (SC, the most active form), was detected on lane 9 (*N*/*P* ratio of 10).

SC bands were observed on lanes 6 (*N*/*P* ratio of 5), 12 (*N*/*P* ratio of 20) and 15 (*N*/*P* ratio of 30), however at higher *N*/*P* ratios (Lanes 12, and 15), most of the plasmid remained protected and bound to the chitosan, because at these high *N*/*P* ratios, the plasmid had difficulties to be released from the oligochitosan after enzymatic incubation. The lack of signal on lane 3 indicates that the enzyme worked properly. After enzymatic treatment, in all the *N*/*P* ratios, the signal of the open circular (OC) form of the plasmid was more intensive than the observed on lane 1 (naked DNA), which indicates partial degradation, since DNase I converts SC form to OC by cutting one of the DNA double strands.

Based on data obtained of particle size, zeta potential and on agarose gel electrophoresis assays, we evaluated *in vitro* the cell viability and the transfection efficiency of polyplexes at *N*/*P* ratios of 10, 20 and 30 on HEK-293 and ARPE-19 cells, at two pH values, 7.4 and 7.1, since this pH value is similar to that found in the vitreous humor of the rat (Bassnett and Duncan, 1985).

As observed in Fig. 4A (bars), the transfection efficiency of polyplexes drastically increased when the pH of the medium slightly decreased from 7.4 to 7.1, reaching significant statistical differences at all *N*/*P* ratios studied. Such increase in transfection efficiency has been attributed to the highly protonated amine groups of the chitosan at low pH values, which enhances the binding affinity to negatively charged phosphate groups of the DNA (Koping-Hoggard et al., 2003; Nimesh et al., 2010; Sato et al., 2001), and facilitates the DNA approach and uptake through the cell membrane during transfection (Dias et al., 2002). Highest EGFP expression was observed at *N*/*P* ratio of 10. For all ratio and pH values studied, cell viability was always over 90% (Fig. 4A lines), which indicates a very low toxic effect of the polyplexes on these cells (Lee et al., 2001).

It has been reported that cultured ARPE-19 cells are well tolerated when exposed to chitosan formulations (Lai et al., 2010), but are more difficult to be transfected than HEK-293 cells (Del Pozo-Rodriguez et al., 2008). In our *in vitro* experiments, we did not find significant transfection efficiency at pH 7.4 and 7.1 in ARPE-19 cells when polyplexes were applied at *N*/*P* ratios of 10, 20 and 30. However, viability values were over 90% in all cases, and flow cytometry FSC/SSC dot plots showed a homogeneous cell population (data not shown). Based on the low cytotoxic effect observed by our formulation, on the lack of a consistent correlation reported between *in vitro* and *in vivo* experiments (Conley and Naash, 2010; Gorman et al., 1997), and on the extended evidence that transfection efficiency significantly varies among different cell lines (Gebhart and Kabanov, 2001), we administered intravitreally and subretinally oligochitosan polyplexes at *N*/*P* ratios of 10 and 30 to Sprague Dawley rats in order to evaluate the transfection efficiency in different layers and cells of the retina.

We selected the subretinal and intravitreal administration injections because they are the most effective ways to deliver material to the posterior segment of the eye, and are clinically viable options (Conley and Naash, 2010). In addition, each route is indicated for a particular purpose, and target cells may be different. While the effect of subretinal injection is generally localized around the injection site, intravitreal injections can carry the delivered material to a larger retinal surface (Dureau et al., 2000).

After subretinal administrations of polyplexes at *N*/*P* ratio of 10, most of the transfection was localized in the external segments of the photoreceptors and in the RPE layer, but not in the inner layers of the retina (Fig. 5B and C). Transfection at this level of the retina could be of great interest to treat many monogenetic or complex retinal dystrophies that are major causes of vision loss worldwide such as age-related macular degeneration and retinitis pigmentosa (Conley and Naash, 2010; Edwards et al., 2005). After intravitreal administration of polyplexes at the same *N*/*P* ratio, transfected cells were more uniformly distributed mainly in the inner layers of the retina (Fig. 6A–C), which suggests a partial diffusion of polyplexes to the whole retina. Probably, the low expression obtained at *N*/*P* 30 could be explained by the electrostatic interactions between the negatively charged glycosaminoglycans present in the vitreous (Clark et al., 2011), and the positively charged administered polyplexes, which would generate aggregates that impede the transport towards the target cell and limit the cellular uptake. The significant expression of the reporter gene in the inner layers of the retina could be of great interest to treat some genetic pathologies of the retina such as the X linked juvenile retinoschisis disease (Delgado et al., 2012). Surprisingly, after intravitreal administrations, we also found transfected cells in the outer segment of the photoreceptors and in the RPE (Fig. 6B and C). Therefore, intravitreal injections of polyplexes based on oligochitosans could be an interesting and promising approach to target the outer retina, since it is easier and safer than subretinal route, although the transgene can be distributed through the trabecular meshwork (Conley and Naash, 2010).

In similarity to other reports, plasmid DNA did not transfect retinal cells after subretinal or intravitreal administrations (Cai et al., 2010; Dezawa et al., 2002) (data not shown). Regarding toxicity, no deleterious effects on retinal cells were observed when polyplexes were administered by both routes. However, other authors reported some important retinal degeneration in chitosan-treated eyes after subretinal administration (Prow et al., 2008), which was attributed to the presence of contaminants in the low grade chitosan formulations employed. In our case, our ultrapure oligochitosans had endotoxin levels <0.05 EU/mg. This is particularly important, since ultrapure chitosans are essentially not toxic, while the toxicity of low grade chitosan is low, but still detectable (Koping-Hoggard et al., 2001). In addition, there are other factors that affect to the toxicity of the polyplexes on retinal cells such as size, concentration, and surface charge (Jo et al., 2011).

5. Conclusion

Our study shows for the first time that polyplexes based on NOVAFECT O25 oligochitosans can transfect different cells of the rat retina efficiently depending on the administration route. Subretinal administrations transfected mainly the pigmented cells of the retinal epithelium and the light sensitive photoreceptor cells, whereas intravitreal injections transfected the inner layers of the retina, retinal ganglion cells, and surprisingly photoreceptors and cells of the RPE. These results support the potential use of oligoch-

itosans for delivering genetic material into retinal cells; however, further studies are required to explore the properties of this material as gene carrier. Smart chemical modifications with appropriate ligands attached to the main block of the oligochitosans could results in more specific and more efficient materials. In addition, a long-term and persistent transgene expression would be desirable for the treatment of genetic or inherited retinal diseases with non-viral vectors.

Acknowledgments

This project was partially supported by the University of the Basque Country UPV/EHU (UFI 11/32), by the Research Chair in Retinitis Pigmentosa "Bidons Egara", and by the National Organization of Spanish Blind People (ONCE). Technical and human support provided by SGIker (UPV/EHU) is gratefully acknowledged.

References

Alatorre-Meda, M., Taboada, P., Hartl, F., Wagner, T., Freis, M., Rodriguez, J.R., 2011. The influence of chitosan valence on the complexation and transfection of DNA: the weaker the DNA-chitosan binding the higher the transfection efficiency. Colloids Surf. B 82, 54–62.

Bainbridge, J.W., Smith, A.J., Barker, S.S., Robbie, S., Henderson, R., Balaggan, K., Viswanathan, A., Holder, G.E., Stockman, A., Tyler, N., Petersen-Jones, S., Bhattacharya, S.S., Thrasher, A.J., Fitzke, F.W., Carter, B.J., Rubin, G.S., Moore, A.T., Ali, R.R., 2008. Effect of gene therapy on visual function in Leber's congenital amaurosis. N. Engl. J. Med. 358, 2231–2239.

Bassnett, S., Duncan, G., 1985. Direct measurement of pH in the rat lens by ion-sensitive microelectrodes. Exp. Eye Res. 40, 585–590.

Bejjani, R.A., BenEzra, D., Cohen, H., Rieger, J., Andrieu, C., Jeanny, J.C., Gollomb, G., Behar-Cohen, F.F., 2005. Nanoparticles for gene delivery to retinal pigment epithelial cells. Mol. Vis. 11, 124–132.

Bivas-Benita, M., Romeijn, S., Junginger, H.E., Borchard, G., 2004. PLGA-PEI nanoparticles for gene delivery to pulmonary epithelium. Eur. J. Pharm. Biopharm. 58, 1–6.

Cai, X., Conley, S.M., Nash, Z., Fliesler, S.J., Cooper, M.J., Naash, M.I., 2010. Gene delivery to mitotic and postmitotic photoreceptors via compacted DNA nanoparticles results in improved phenotype in a mouse model of retinitis pigmentosa. FASEB J. 24, 1178–1191.

Charbel Issa, P., MacLaren, R.E., 2012. Non-viral retinal gene therapy: a review. Clin. Experiment Ophthalmol. 40, 39–47.

Cideciyan, A.V., Aleman, T.S., Boye, S.L., Schwartz, S.B., Kaushal, S., Roman, A.J., Pang, J.J., Sumaroka, A., Windsor, E.A., Wilson, J.M., Flotte, T.R., Fishman, G.A., Heon, E., Stone, E.M., Byrne, B.J., Jacobson, S.G., Hauswirth, W.W., 2008. Human gene therapy for RPE65 isomerase deficiency activates the retinoid cycle of vision but with slow rod kinetics. Proc. Natl. Acad. Sci. USA 105, 15112–15117.

Clark, S.J., Keenan, T.D., Fielder, H.L., Collinson, L.J., Holley, R.J., Merry, C.L., van Kuppevelt, T.H., Day, A.J., Bishop, P.N., 2011. Mapping the differential distribution of glycosaminoglycans in the adult human retina, choroid, and sclera. Invest. Ophthalmol. Vis. Sci. 52, 6511–6521.

Conley, S.M., Naash, M.I., 2010. Nanoparticles for retinal gene therapy. Prog. Retin Eye Res. 29, 376–397.

Danielsen, S., Varum, K.M., Stokke, B.T., 2004. Structural analysis of chitosan mediated DNA condensation by AFM: influence of chitosan molecular parameters. Biomacromolecules 5, 928–936.

del Pozo-Rodriguez, A., Delgado, D., Solinis, M.A., Gascon, A.R., Pedraz, J.L., 2008. Solid lipid nanoparticles for retinal gene therapy: transfection and intracellular trafficking in RPE cells. Int. J. Pharm. 360, 177–183.

Delgado, D., Del Pozo-Rodriguez, A., Solinis, M.A., Aviles, M., Weber, B.H., Fernandez, E., Rodriguez Gascon, A., 2012. Dextran and protamine-based solid lipid nanoparticles as potential vectors for the treatment of X linked juvenile retinoschisis. Hum. Gene. Ther..

Dezawa, M., Takano, M., Negishi, H., Mo, X., Oshitari, T., Sawada, H., 2002. Gene transfer into retinal ganglion cells by in vivo electroporation: a new approach. Micron 33, 1–6.

Dias, R., Antunes, F., Miguel, M., Lindman, S., Lindman, B., 2002. DNA-lipid systems. A physical chemistry study. Braz. J. Med. Biol. Res. 35, 509–522.

Diebold, Y., Calonge, M., 2010. Applications of nanoparticles in ophthalmology. Prog. Retin Eye Res. 29, 596–609.

Dureau, P., Legat, L., Neuner-Jehle, M., Bonnel, S., Pecqueur, S., Abitbol, M., Dufier, J.L., 2000. Quantitative analysis of subretinal injections in the rat. Graefes Arch. Clin. Exp. Ophthalmol. 238, 608–614.

Edwards, A.O., Ritter 3rd, R., Abel, K.J., Manning, A., Panhuysen, C., Farrer, L.A., 2005. Complement factor H polymorphism and age-related macular degeneration. Science 308, 421–424.

Gebhart, C.L., Kabanov, A.V., 2001. Evaluation of polyplexes as gene transfer agents. J. Controlled Release 73, 401–416.

Gorman, C.M., Aikawa, M., Fox, B., Fox, E., Lapuz, C., Michaud, B., Nguyen, H., Roche, E., Sawa, T., Wiener-Kronish, J.P., 1997. Efficient in vivo delivery of DNA to pulmonary cells using the novel lipid EDMPC. Gene. Ther. 4, 983–992.

Hauswirth, W.W., Aleman, T.S., Kaushal, S., Cideciyan, A.V., Schwartz, S.B., Wang, L., Conlon, T.J., Boye, S.L., Flotte, T.R., Byrne, B.J., Jacobson, S.G., 2008. Treatment of leber congenital amaurosis due to RPE65 mutations by ocular subretinal injection of adeno-associated virus gene vector: short-term results of a phase I trial. Hum. Gene. Ther. 19, 979–990.

Huang, M., Fong, C.W., Khor, E., Lim, L.Y., 2005. Transfection efficiency of chitosan vectors: effect of polymer molecular weight and degree of deacetylation. J. Controlled Release 106, 391–406.

Jafari, M., Soltani, M., Naahidi, S., Karunaratne, D.N., Chen, P., 2012. Nonviral approach for targeted nucleic acid delivery. Curr. Med. Chem. 19, 197–208.

Jo, D.H., Lee, T.G., Kim, J.H., 2011. Nanotechnology and nanotoxicology in retinopathy. Int. J. Mol. Sci. 12, 8288–8301.

Johnson, L.N., Cashman, S.M., Kumar-Singh, R., 2008. Cell-penetrating peptide for enhanced delivery of nucleic acids and drugs to ocular tissues including retina and cornea. Mol. Ther. 16, 107–114.

Kiang, T., Wen, J., Lim, H.W., Leong, K.W., 2004. The effect of the degree of chitosan deacetylation on the efficiency of gene transfection. Biomaterials 25, 5293–5301.

Klausner, E.A., Zhang, Z., Chapman, R.L., Multack, R.F., Volin, M.V., 2010. Ultrapure chitosan oligomers as carriers for corneal gene transfer. Biomaterials 31, 1814–1820.

Klausner, E.A., Zhang, Z., Wong, S.P., Chapman, R.L., Volin, M.V., Harbottle, R.P., 2012. Corneal gene delivery: chitosan oligomer as a carrier of CpG rich, CpG free, or S/MAR plasmid DNA. J. Gene. Med. 14, 100–108.

Koping-Hoggard, M., Tubulekas, I., Guan, H., Edwards, K., Nilsson, M., Varum, K.M., Artursson, P., 2001. Chitosan as a nonviral gene delivery system. Structure-property relationships and characteristics compared with polyethylenimine in vitro and after lung administration in vivo. Gene. Ther. 8, 1108–1121.

Koping-Hoggard, M., Mel'nikova, Y.S., Varum, K.M., Lindman, B., Artursson, P., 2003. Relationship between the physical shape and the efficiency of oligomeric chitosan as a gene delivery system in vitro and in vivo. J. Gene. Med. 5, 130–141.

Lai, J.Y., Li, Y.T., Wang, T.P., 2010. In vitro response of retinal pigment epithelial cells exposed to chitosan materials prepared with different cross-linkers. Int. J. Mol. Sci. 11, 5256–5272.

Lee, M., Nah, J.W., Kwon, Y., Koh, J.J., Ko, K.S., Kim, S.W., 2001. Water-soluble and low molecular weight chitosan-based plasmid DNA delivery. Pharm. Res. 18, 427–431.

Liu, M.M., Tuo, J., Chan, C.C., 2011. Gene therapy for ocular diseases. Br. J. Ophthalmol. 95, 604–612.

Maguire, A.M., Simonelli, F., Pierce, E.A., Pugh Jr., E.N., Mingozzi, F., Bennicelli, J., Banfi, S., Marshall, K.A., Testa, F., Surace, E.M., Rossi, S., Lyubarsky, A., Arruda, V.R., Konkle, B., Stone, E., Sun, J., Jacobs, J., Dell'Osso, L., Hertle, R., Ma, J.X., Redmond, T.M., Zhu, X., Hauck, B., Zelenaia, O., Shindler, K.S., Maguire, M.G., Wright, J.F., Volpe, N.J., McDonnell, J.W., Auricchio, A., High, K.A., Bennett, J., 2008. Safety and efficacy of gene transfer for Leber's congenital amaurosis. N. Engl. J. Med. 358, 2240–2248.

Mao, H.Q., Roy, K., Troung-Le, V.L., Janes, K.A., Lin, K.Y., Wang, Y., August, J.T., Leong, K.W., 2001. Chitosan-DNA nanoparticles as gene carriers: synthesis, characterization and transfection efficiency. J. Controlled Release 70, 399–421.

Maurstad, G., Danielsen, S., Stokke, B.T., 2007. The influence of charge density of chitosan in the compaction of the polyanions DNA and xanthan. Biomacromolecules 8, 1124–1130.

Nimesh, S., Thibault, M.M., Lavertu, M., Buschmann, M.D., 2010. Enhanced gene delivery mediated by low molecular weight chitosan/DNA complexes: effect of pH and serum. Mol. Biotechnol. 46, 182–196.

Nussenblatt, R.B., Csaky, K., 1997. Perspectives on gene therapy in the treatment of ocular inflammation. Eye (Lond.) 11 (Pt 2), 217–221.

Prow, T.W., Bhutto, I., Kim, S.Y., Grebe, R., Merges, C., McLeod, D.S., Uno, K., Mennon, M., Rodriguez, L., Leong, K., Lutty, G.A., 2008. Ocular nanoparticle toxicity and transfection of the retina and retinal pigment epithelium. Nanomedicine 4, 340–349.

Rolland, A., 2005. Gene medicines: the end of the beginning? Adv. Drug Deliv. Rev. 57, 669–673.

Sato, T., Ishii, T., Okahata, Y., 2001. In vitro gene delivery mediated by chitosan. Effect of pH, serum, and molecular mass of chitosan on the transfection efficiency. Biomaterials 22, 2075–2080.

Zhang, Y., Schlachetzki, F., Li, J.Y., Boado, R.J., Pardridge, W.M., 2003. Organ-specific gene expression in the rhesus monkey eye following intravenous non-viral gene transfer. Mol. Vis. 9, 465–472.